Journal of Colloid and Interface Science **243,** 382–387 (2001)
doi:10.1006/jcis.2001.7850, available online at http://www.idealibrary.com on IDEAL®

A Self-Assembled Monolayer of an Alkanoic Acid-Derivatized Porphyrin on Gold Surface: A Structural Investigation by Surface Plasmon Resonance, Ultraviolet–Visible, and Infrared Spectroscopies

Zhijun Zhang,* Naofumi Yoshida,* Toyoko Imae,*,[1] Qingbin Xue,† Ming Bai,† Jianzhuang Jiang,† and Zhongfan Liu‡

*Research Center for Materials Science (RCMS), Nagoya University, Chikusa, Nagoya 464-8602, Japan; †Department of Chemistry, Shandong University, Jinan, Shandong 250100, People's Republic of China; and ‡Center for Nanoscale Science and Technology (CNST), College of Chemistry and Molecular Engineering, Peking University, Beijing 100871, People's Republic of China

Received May 21, 2001; accepted July 14, 2001; published online October 5, 2001

We describe in this paper the preparation of a self-assembled monolayer (SAM) film of 5,10,15,20-tetra(*N*-10-carboxydecyl-pyridinium-4-yl) porphyrin on an Au substrate by chemisorption of the multi-COOH terminal groups onto the metal surface. A film thickness of 19 Å is deduced from surface plasmon resonance measurement. A significant red shift of the Soret band in the UV–vis spectrum of the porphyrin SAM compared with that of the porphyrin in solution suggests the formation of "head-to-tail" type aggregates in the SAM. The absence of the N–H in-plane mode and the presence of the out-of-plane mode in the infrared reflection-absorption spectrum (IRAS) and the surface-enhanced infrared absorption spectrum (SEIRAS) further suggest that the porphyrin macrocycle is oriented flatly with respect to the surface of the metal substrate. In addition, there may be one of the four acid groups that is unbound to the metal surface, as evidenced by the presence of a very weak band at 1707 cm^{-1} due to the C=O stretching mode of the COOH group in the SEIRA spectrum of the porphyrin monolayer on the Au island film.

INTRODUCTION

Recently we (1) have observed that protoporphyrin IX Zinc (II), a porphyrin with two COOH groups, can form a stable self-assembled monolayer (SAM) film on a gold surface by deprotonation of the COOH group and formation of COO^- bound to the metal surface. As an extension of our previous work, we report herein a new type of SAM of a porphyrin substituted by four alkanoic COOH groups. A careful design of the porphyrin structure was made to prepare the SAM in which the porphyrin plane assumes a known orientation. It is well known that a controlled orientation of the ultrathin porphyrin solid films is of practical significance for their applications in many fields, such as development of porphyrin-based molecular devices and surface catalysis (2–6).

There are two main methods of preparing SAMs of porphyrin with a controlled orientation: (1) chemisorption of alkylthiol-linked porphyrins to a metal surface, developed by Zak *et al*. (3) and Hutchison and colleagues (4–6), and (2) axial ligation of metalloporphyrins to a ligand-modified surface, described for the first time by Li *et al*. (7) and later developed by Offord *et al*. (8) and others (9–12). The new method to be presented here belongs to the first category, but the synthesis of the film-forming material is much easier than the methods described previously (3–6).

Formation and organization of the SAM film of the porphyrin, 5,10,15,20-tetra(*N*-10-carboxydecyl-pyridinium-4-yl) porphyrin (TCPyP), the structure of which is shown in Fig. 1, were studied by means of surface plasmon resonance (SPR), ultraviolet–visible (UV–vis), normal infrared reflection–absorption (IRA), and surface-enhanced infrared absorption (SEIRA) spectroscopies. Among the surface analytical tools employed, the newly developed SEIRA spectroscopy gives IR bands with signal-to-noise ratios much higher than those of normal IRAS and, therefore, is very suitable for the structural characterization of surface monolayer films (13).

EXPERIMENTAL

Film-Forming Material and Reagents

The porphyrin, TCPyP, was synthesized by alkylation of 5,10,15,20-tetra(4-pyridyl)porphyrin (TPyP) with 10-Br-1-decanoic acid and purified according to the literature (14). Other reagents used in the experiment are of reagent grade. Milli-Q ultrapure water (>18.2 MΩ cm) was used throughout the experiment.

Substrate Preparation

Gold-evaporated glass substrates used for SPR and IRAS measurements were commercially available, and the thickness of the gold layer was 45 and 250 nm, respectively. The Au substrates were cleaned with "piranha solution," described previously (15), prior to the formation of the porphyrin adlayer. Au

[1] To whom correspondence should be addressed. Fax: +81-52-789-5912. E-mail: imae@nano.chem.nagoya-u.ac.jp.

0021-9797/01 $35.00

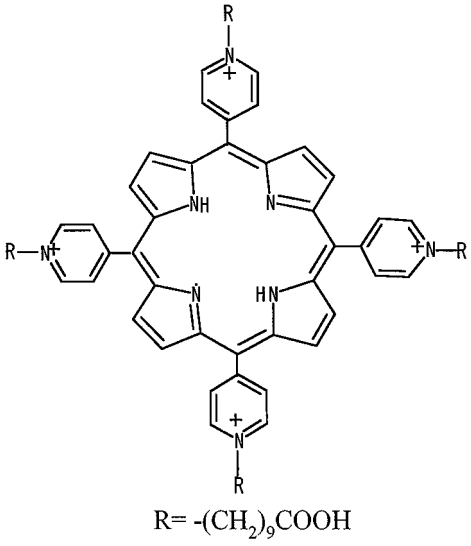

FIG. 1. Chemical structure of 5,10,15,20-tetra(*N*-10-carboxydecyl-pyridinium-4-yl)porphyrin (TCPyP).

substrates used for UV–vis transmission and SEIRA measurements were prepared as follows: glass plates were cleaned with "piranha solution" following typical procedure. The Au island films, 15 nm thick, were then thermally evaporated onto the precleaned glass substrates at 1×10^{-6} Torr. The Au island films thus prepared were used immediately for the formation of the porphyrin monolayer films and for the measurement of the transmission UV–vis spectra and IR spectra in reflection–absorption mode.

SAM Formation

The cleaned glass slides or freshly prepared gold substrates were soaked in an aqueous 1.0×10^{-4} M solution of TCPyP for 24 h. They were then rinsed thoroughly with plentiful amounts of ethanol. Although the gold substrates with the porphyrins were used immediately for spectral measurement, the glass substrates coated with the porphyrins were further sonicated twice for 3 min and washed again before spectral measurement to remove physisorbed species.

SPR Spectroscopy

The SPR spectrum was recorded at 30°C with a Biosensor Analytical System (Nippon Laser & Electronics Lab). An aqueous solution of TCPyP was filled in a solution cell on an Au-evaporated glass substrate. The SPR reflectance angle shift under 670-nm laser light was monitored as a function of adsorption time until adsorption equilibrium was reached. The reflectance versus incidence angle curve was taken at equilibrium adsorption. The curve was fitted to standard Fresnel theory (16) for the four-layer model. The thickness of the porphyrin adlayer was then evaluated, and the angle shift versus adsorption time curve was calculated.

UV–Vis Spectroscopy

Measurements of UV–vis transmission spectra were carried out with a Shimadzu UV-2200 spectrophotometer. The UV–vis spectra of TCPyP film were obtained for two films of the porphyrin, which are adsorbed on the Au island film and on the glass side. Then the UV–vis spectrum of the TCPyP film formed on the Au island film can be obtained by subtracting half of the UV–vis spectrum of the TCPyP on a glass substrate (with porphyrin films formed on both sides of the glass) from the spectrum of the TCPyP film on the Au island film.

IRA and SEIRA Spectroscopies

All IR spectra were recorded on a Bio-Rad FTS 575C FT-IR spectrometer equipped with a liquid nitrogen-cooled MCT detector. The IR spectra were collected with 1024 scans at 4 cm^{-1}. The IRA and SEIRA spectra were measured using a Harrick reflectance attachment with an incidence angle of 75°. The spectra of the porphyrin monolayer films were ratioed to a background spectrum of a bare Au substrate before deposition of the porphyrin SAM.

RESULTS AND DISCUSSION

SPR Spectra

SPR spectroscopy is widely used to investigate adsorption dynamics and to determine the thickness of surface monolayer films (17–21). Figure 2A shows SPR curves (reflectance versus incident angle) of an Au substrate (a) before and (b) after the formation of TCPyP monolayer film at the equilibrium state of the adsorption. Curve b shows a small but meaningful shift compared with curve a, suggesting the presence of an adlayer of TCPyP on the Au surface. More useful information on the adsorption nature can be obtained if we plot the adlayer thickness as a function of the adsorption time, which is shown in Fig. 2B. It is clearly seen that the thickness is steeply increased at the initial stage, implying rapid adsorption kinetics. The thickness then becomes nearly constant with increases in the adsorption time, which indicates attainment of adsorption equilibrium.

From the SPR spectrum, the thickness of the porphyrin film was determined to be 19 ± 2 Å at the equilibrium state. To verify whether the porphyrin adlayer is physisorbed or chemisorbed on the Au substrate, and further to check whether the thickness of the adlayer corresponds to that of a monolayer or a multilayer, an desorption experiment was carried out by rinsing the porphyrin-adsorbed Au substrate with water. No noticeable change in the reflectance angle shift was observed with the desorption process, indicating chemisorption of the porphyrin on the Au surface.

The length of the COOH-terminated alkyl chain ($-(CH_2)_9$ COOH) is about 14 Å, if the alkyl chain takes the all-*trans* conformation (22). The thickness and the diameter of TPyP are estimated to be roughly 5 and 17 Å, respectively, similar to those of 5,10,15,20-tetraphenylporphyrin (23, 24). The thickness of the TCPyP monolayer film is then expected to be about 20 Å, if

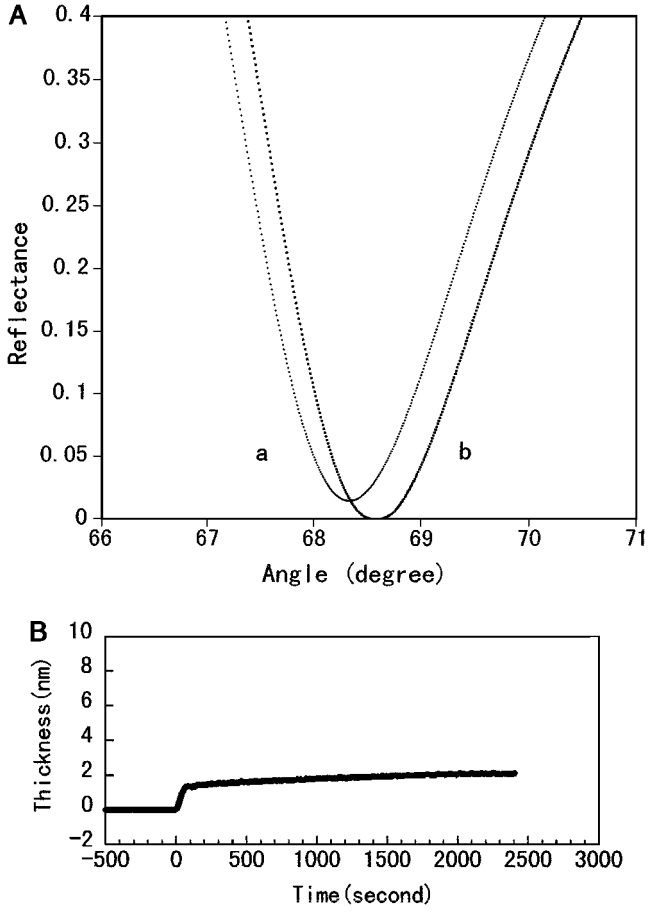

FIG. 2. (A) SPR spectra of an Au substrate (a) before and (b) after adsorption of TCPyP. (B) A plot of adlayer thickness as a function of adsorption time from an aqueous solution of TCPyP (1.0×10^{-4} M).

the porphyrin is bound to the Au substrate via chemisorption of the COOH groups to the Au surface. This results in a coplanar orientation of the porphyrin plane with the metal surface. The film thickness calculated is in good agreement with that evaluated from the SPR data. It is very unlikely that the porphyrin plane is in vertical orientation or the remarked tilt with respect to the Au surface, because in this case the thickness of the film would reach 40 Å or even larger. The coplanar orientation of the porphyrin macrocycle with the Au surface is further supported by our UV–vis and IR experiments, as discussed below.

UV–Vis Spectra

Figure 3 presents UV–vis transmission spectra of an aqueous solution of TCPyP and a SAM of TCPyP on an Au island film. The solution shows a strong band (the Soret band) at 425 nm and four small bands (Q bands) in the region between 500 and 700 nm, which are typical of a free base porphyrin. The SAM gives significant broadening (full width at half height (FWHH) 41.3 nm) and red shift (441 nm) of the Soret band, compared to the solution (FWHH 26 nm, 425 nm). These facts suggest the formation of "head-to-tail" type aggregates (3, 24, 25) in the SAM. That is, each porphyrin molecule takes a nearly flat orientation with respect to the metal surface in the SAM. It is very unlikely that a "face-to-face" or "edge-to-edge" type aggregate occurs, since such aggregation usually yields a blue shift or splitting of the Soret band (25–29). The IR data to be discussed below provide further evidence supporting the flatter orientation of the porphyrin molecule to the Au surface.

IR Spectra

The SEIRA (a) and IRA (b) spectra in the regions from 4000 to 2500 cm^{-1} and from 1900 to 680 cm^{-1} of the SAM of TCPyP are presented in Figs. 4A and 4B, respectively. For the purpose of comparison, an IR spectrum of the TCPyP solid in KBr pellet is also added in Fig. 4. The main bands appearing in the KBr spectrum were assigned on the basis of previous literature (25b, 30, 31).

In spectrum c of Fig. 4, a broad and strong band at 3433 cm^{-1} arises mainly from the O–H stretching mode of water molecules bound to the cationic porphyrin. A band due to the stretching mode of the N–H group of the porphyrin is barely resolved at about 3319 cm^{-1} as a shoulder on the low-wavenumber side of the broad band at 3433 cm^{-1}. Besides this high-wavenumber band, two bands at 970 and 723 cm^{-1} due to N–H in-plane and out-of-plane bending modes, respectively, also appear in the low-wavenumber region. A strong band at 2924 cm^{-1} and a medium band at 2853 cm^{-1} are ascribed to CH_2 antisymmetric and symmetric stretching modes, respectively, of the long alkyl chain. The C=O stretching mode of the COOH group attached to the alkyl chain gives rise to a moderate band at 1719 cm^{-1}. A strong band located at 1637 cm^{-1} is ascribed to the C=N stretching mode of the pyridinium group. Some weak and medium bands due to the vibrational modes of the porphyrin ring and to the substituted pyridyl and alkyl chains also appear in the region 1600–680 cm^{-1} of the solid spectrum.

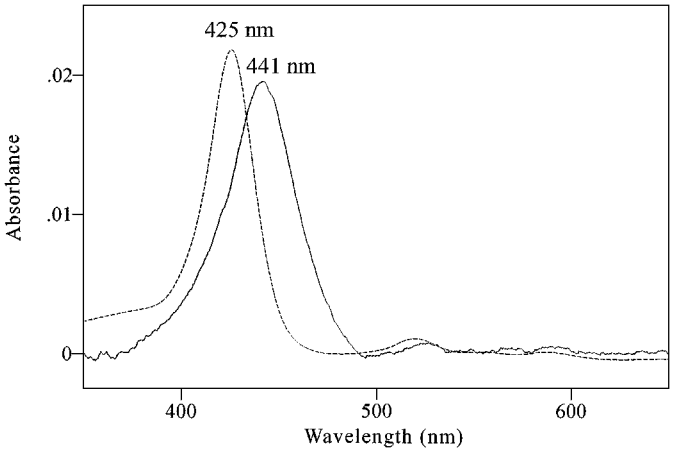

FIG. 3. UV–vis transmission spectra of TCPyP in a SAM on gold substrate (solid line) and in an aqueous solution (a.u.) (dashed line).

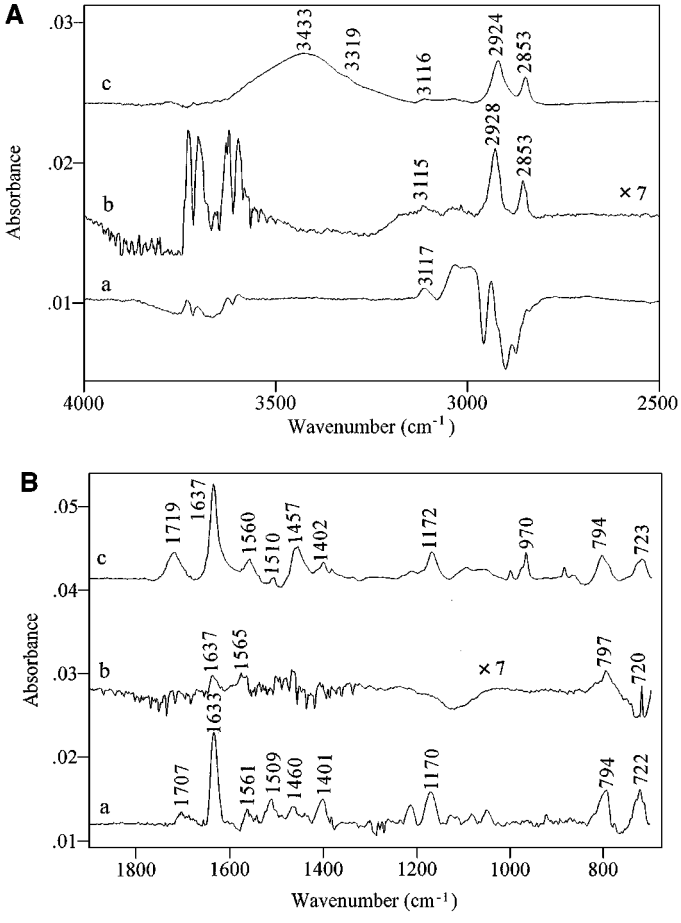

FIG. 4. (A) (a) SEIRAS and (b) IRA spectra in the region 4000–2500 cm^{-1} of a SAM of TCPyP on an Au island film and thick Au, respectively. A transmission IR spectrum of TCPyP solid dispersed in a KBr pellet (a.u.) is shown as spectrum c. (B) As in part A but in the region 1900–680 cm^{-1}.

The comparison of spectra of the porphyrin in SAM and in KBr disk provides important structural information for the porphyrin SAM. There are several important differences in the SAM and solid spectra. First, two bands at 3319 and 970 cm^{-1}, due to the in-plane stretching and bending modes of the N-H group of the porphyrin ring, are completely missed in the SEIRAS and IRAS, whereas the band due to the out-of-plane bending mode of the N-H group still appears at 720 and 722 cm^{-1} in the IRAS and SEIRAS, respectively. According to the surface selection rules of IRAS and SEIRAS, only vibrations that have dipole moments perpendicular to the metal surface or the local surfaces of the metal islands give IR absorption (13). Therefore, the absence of the two bands at 3319 and 970 cm^{-1} due to the in-plane vibration modes and the presence of the band at ~720 cm^{-1} due to the out-of-plane bending mode of the N-H group strongly suggest that the porphyrin plane takes a flat orientation with respect to the metal surface. This result is well consistent with our SPR and UV–vis spectral results presented above.

The second feature is that the C=O band, which appears at 1719 cm^{-1} at a medium intensity in the solid spectrum, is at 1707 cm^{-1} and becomes very weak in the SEIRAS, although it is unresolved in the IRAS because of a low S/N ratio. In contrast, the medium band at 1401 cm^{-1} due to the symmetric stretching mode of the COO^- appears in the SEIRAS. These facts are consistent with the formation of a COO^- species by chemisorption of COOH groups onto the metal surface. Few COOH groups coexist with COO^- groups in the SAM. It is likely from the absorbance ratio of COOH and COO^- bands that three COO^- groups are bound to the Au surface, while only one COOH remains unbound. As discussed in the UV–vis spectra section, the porphyrins formed "head-to-tail" type aggregates where neighboring porphyrin molecules came close to each other through the side with COOH unbound to the surface. In the meantime, the unbound COOH group forms a hydrogen bond with that of the other porphyrin, as expected from the low wavenumber.

Third, two bands due to the CH_2 antisymmetric and symmetric stretching modes of the alkyl chain appear in the IRAS. It is suggested from the surface selection rule that the alkyl chain axes are tilted significantly with respect to the metal surface. The band positions at 2928 and 2853 cm^{-1} in the IRAS vary from those for highly ordered chains (*trans*-zigzag conformation) (32). The upward shifts in wavenumber imply an increase in the conformational disorder, i.e., the *gauche* conformers in the hydrocarbon chain in the porphyrin SAM. This phenomenon is easy to understand if we consider that (1) a CH_2 unit attached directly to the pyridyl group and the neighboring CH_2 groups may take gauche

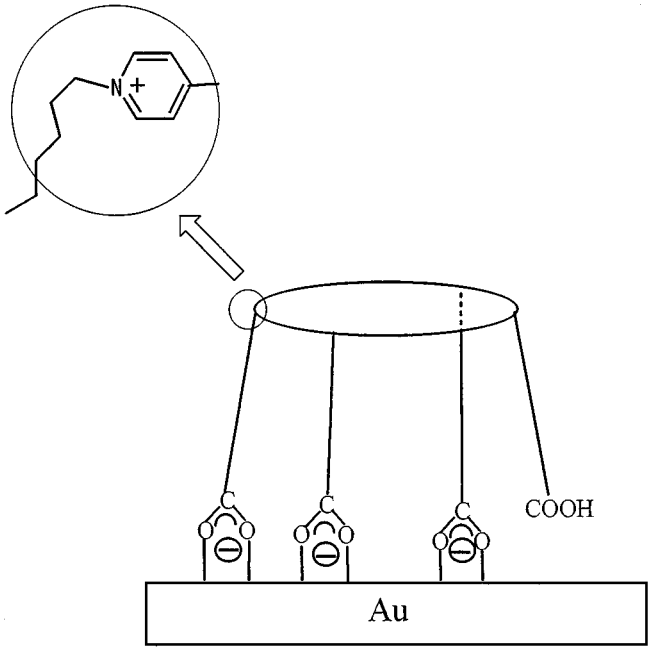

FIG. 5. A proposed model showing the structure of TCPyP in a SAM on an Au surface.

conformations in the SAM and (2) each alkyl chain cannot pack densely and orderly because the porphyrin moiety has a rather large space (calculated area per porphyrin macroplane is about 200 $Å^2$) to accommodate four alkanoic acid groups (four COOH groups occupy a total area of about 20 $Å^2 \times 4 = 80$ $Å^2$) (25b).

It should be noted that bands due to stretching modes of the alkyl groups in the high-wavenumber region (3000–2800 cm^{-1}) are distorted severely in the SEIRAS. The bare Au island, which serves as a background to gain a spectrum of SAM, strongly adsorbs hydrocarbon contaminants from the air prior to the formation of SAM (33). The problem is not so serious in the case of IRAS. Therefore, for the observation of bands in the high wavenumber region, IRAS seems better. The SEIRAS, however, exhibits bands in the low wavenumber region with a much higher S/N ratio than IRAS.

The fourth remarked feature is that the strong and broad band at 3433 cm^{-1} in the solid spectrum disappears completely in the IRAS and SEIRAS. This indicates that the large amount of water molecules bound to the cationic porphyrin solid became much less in the monolayer film.

On the basis of the SPR, UV–vis, and IR results discussed above, we propose a schematic model showing the structure of the TCPyP molecule in the monolayer film on the Au surface, as presented in Fig. 5.

CONCLUSION

By intentional design of the porphyrin structure, good control of the porphyrin orientation with respect to the metal surface in the SAM was achieved. The flat orientation of the macrocycle of alkanoic acid-derivatized porphyrin in the SAM was confirmed by SPR, UV–vis, and IR experiments.

The monolayer films of porphyrins with controlled orientation provide an ideal template to probe the catalytic (3–6) and DNA-binding (34, 35) properties of the porphyrins. More importantly, by inserting different metals into the porphyrin (36) and then choosing a suitable bifunctional ligand, we can form multilayer films with a known orientation of each component (8), which are promised as constituents of molecular devices. It should be mentioned that alkanoic acid-derivatized porphyrins can also form SAMs on surfaces of many other substrates, such as glass (37), including Ag (oxide) (38), Al (oxide) (39), porous Si (40), and TiO_2 (41). These porphyrin SAM-coated films will find their applications in many fields.

ACKNOWLEDGMENT

Z.Z. is grateful to the Japan Society for the Promotion of Science (JSPS) for a postdoctoral fellowship.

REFERENCES

1. Zhang, Z.-J., and Imae, T., *Nano Lett.* **1,** 241 (2001).
2. Bardwell, J. A., and Bolton, J. R., *Photochem. Photobiol.* **40,** 319 (1984).
3. Zak, J., Yuan, H. P., Ho, M., Woo, L. K., and Porter, M. D., *Langmuir* **9,** 2772 (1993).
4. Hutchison, J. E., Postlehwaite, T. A., and Murray, R. W., *Langmuir* **9,** 3277 (1993).
5. Postlehwaite, T. A., Hutchison, J. E., Hathcock, K. W., and Murray, R. W., *Langmuir* **11,** 4109 (1995).
6. Hutchison, J. E., Postlehwaite, T. A., Chen, C.-H., Hathcock, K. W., Ingram, R. S., Ou, W., Linton, R. W., and Murray, R. W., *Langmuir* **13,** 2143 (1997).
7. Li, D., Moore, L. W., and Swanson, B. I., *Langmuir* **10,** 1177 (1994).
8. Offord, D. A., Sachs, S. B., Ennis, M. S., Eberspacher, T. A., Griffin, J. H., Chidsey, C. E. D., and Collman, J. P., *J. Am. Chem. Soc.* **120,** 4478 (1998).
9. Ashkenasy, G., Kalyuzhny, G., Libman, J., Rubinstein, I., and Shanzer, A., *Angew. Chem. Int. Ed. Engl.* **38,** 1257 (1999).
10. Da Cruz, F., Driaf, K., Berthier, C., Lameille, J.-M., and Armand, F., *Thin Solid Films* **349,** 155 (1999).
11. Huc, V., Bourgoin, J. P., Bureau, C., Valin, F., Zalczer, G., and Palacin, S., *J. Phys. Chem.* **103,** 10489 (1999).
12. Zhang, Z.-J., Hou, S. F., Zhu, Z. H., and Liu, Z. F., *Langmuir* **16,** 537 (2000).
13. (a) Osawa, M., *Bull. Chem. Soc. Jpn.* **70,** 2861 (1997), and references cited therein. (b) Aroca, R., and Price, B., *J. Phys. Chem. B* **101,** 6537 (1997). (c) Imae, T., and Torii, H., *J. Phys. Chem. B* **104,** 9218 (2000). (d) Zhang, Z.-J., and Imae, T., *J. Colloid Interface Sci.* **233,** 99 (2001).
14. Dancil, K. P. S., Hilario, L. F., Khoury, R. G., Mai, K. U., Nguyen, C. K., Weddle, K. S., and Schachter, A. M., *J. Heterocycl. Chem.* **34,** 749 (1997).
15. Zhang, Z.-J., Hu, R. S., and Liu, Z. F., *Langmuir* **16,** 1158 (2000).
16. Tompkins, H. G., and McGahan, W. A., "Spectroscopic Ellipsometry and Reflectometry." Wiley, New York, 1999.
17. Jung, L. S., Campbell, C. T., Chinowsky, T. M., Mar, M. N., and Yee, S. S., *Langmuir* **14,** 5636 (1998).
18. Lahiri, J., Isacs, L., Grzybowski, B., Carbeck, J. D., and Whitesides, G. M., *Langmuir* **15,** 7186 (1999).
19. Auer, F., Sellergren, B., Swietlow, A., and Offenhauser, A., *Langmuir* **16,** 5936 (2000).
20. Cassagneau, T., Guerin, F., and Fendler, J. H., *Langmuir* **16,** 7318 (2000).
21. Imae, T., Ito, M., Aoi, K., Tsutsumiuchi, K., Noda, H., and Okada, M., *Colloid Surf. A Physicochem. Eng. Aspects* **175,** 225 (2000).
22. Ulman, A., "An Introduction to Ultrathin Organic Films, From Langmuir-Blodgett Films to Self-Assembly." Academic Press, San Diego, 1991.
23. Mangaani, S., Edgar, F., Meyer, J., Cullen, D. L., Tsutsumi, M., and Carrano, C. J., *Inorg. Chem.* **22,** 400 (1983).
24. Boeckl, M. S., Bramblett, A. L., Hauch, K. D., Sasaki, T., Ratner, B. D., and Rogers, J. W., Jr., *Langmuir* **16,** 5644 (2000).
25. (a) Schenning, A. P. H. G., Hubert, D. H. W., Feisters, M. C., and Nolte, R. J. M., *Langmuir* **12,** 1572 (1996). (b) Zhang, Z.-J., Verma, A. L., Yoneyama, M., Nakashima, K., Iriyama, K., and Ozaki, Y., *Langmuir* **13,** 4422 (1997).
26. Gouterman, H., Hanson, L. K., Khalil, G.-E., Buchler, J. W., Rohbock, K., and Dolphin, D., *J. Am. Chem. Soc.* **97,** 3142 (1975).
27. Osuka, A., and Murayama, K., *J. Am. Chem. Soc.* **110,** 4454 (1988).
28. Schick, G. A., Schreiman, I. C., Wagner, R. W., Lindsey, J. S., and Bocian, D. F., *J. Am. Chem. Soc.* **111,** 1344 (1989).
29. Araki, K., Wagner, M. J., and Wrighton, M. S., *Langmuir* **12,** 5393 (1996).
30. (a) Mason, S. F., *J. Chem. Soc.* 976 (1958). (b) Thomas, D. W., and Martell, A. E., *J. Am. Chem. Soc.* **81,** 5111 (1958). (c) Ogoshi, H., Saito, Y., and Nakamoto, K., *J. Chem. Phys.* **57,** 4194 (1972).
31. Li, D., Swanson, B. I., Robinson, J. M., and Hoffbauer, M. A., *J. Am. Chem. Soc.* **115,** 6975 (1993).

32. Myrzakozha, D. A., Hasegawa, T., Nishijo, J., Imae, T., and Ozaki, Y., *Langmuir* **15,** 3601 (1999), and references cited therein.
33. Osawa, M., and Ikeda, M., *J. Phys. Chem.* **95,** 9914 (1991).
34. Gibbs, E., Tinacio, I., Maestre, M., Ellinas, P., and Pasternack, R., *Biochem. Biophys. Res. Commun.* **157,** 350 (1988).
35. Mukunddan, N., Petho, G., Dixon, D., Kim, M., and Marzilli, L., *Inorg. Chem.* **33,** 4676 (1994).
36. Schmehl, R. H., Shaw, G. L., and Whitten, D. G., *Chem. Phys. Lett.* **58,** 549 (1978).
37. Zhang, Z.-J., and Imae, T., unpublished results.
38. (a) Schlotter, N. E., Porter, M. D., Bright, T. B., and Allara, D. L., *Chem. Phys. Lett.* **132,** 93 (1986). (b) Smith, E. L., and Porter, M. D., *J. Phys. Chem.* **97,** 8032 (1993). (c) Tao, Y. T., Lee, M. T., and Chang, S. C., *J. Am. Chem. Soc.* **115,** 9547 (1993).
39. Allara, D. L., Dubois, L. H., and Nuzzo, R. G., *Langmuir* **1,** 45 (1985). (b) Allara, D. L., and Nuzzo, R. G., *Langmuir* **1,** 52 (1985).
40. Lee, E. J., Ha, J. S., and Sailor, M. J., *J. Am. Chem. Soc.* **117,** 8295 (1995).
41. Cherian, S., and Wamser, C. C., *J. Phys. Chem. B* **104,** 3624 (2000).